3D Printed One-shot Deployable Flexible "Kirigami" Dielectric Reflectarray Antenna for mm-Wave Applications

Yepu Cui, Syed Abdullah Nauroze, Ryan Bahr, Emmanouil M. Tentzeris
School of Electrical and Computer Engineering, Georgia Institute of Technology, USA
yepu.cui@gatech.edu, nauroze@gatech.edu, rbahr3@gatech.edu, etentze@ece.gatech.edu

***Abstract*— This paper presents a first-of-its-kind fully 3D-printed mm-wave reflectarray with one-shot deployability. It consists of an array of kirigami-inspired flat-foldable dielectric-based unit cells featuring an unprecedented reduction in volume as compared to its conventional counterparts. The prototype is fabricated with high-resolution stereolithography 3D printing together with flexible photosensitive resin. The outcome of this work demonstrates a low-cost, high-performance dielectric reflectarray design that can be folded to 1/3 of the full-scale volume which can be used for outer-space, 5G and various other terrestrial applications.**

***Keywords*— 3D printing, additive manufacturing, antenna arrays, dielectric resonate antennas, flexible electronics, kirigami, origami, reflectarrays.**

I. Introduction

Parabolic and phased array antennas are two of the most widely used high gain antennas in traditional long range and mm-wave communication systems. However, parabolic antennas are bulky, expensive, occupy large space and hard to realize especially at mm-wave frequencies due to their curved profile. Similarly, while phased array antennas feature a planar profile, they require a feeding circuit with phase shifters and power amplifiers that drastically increase their cost. In contrast, reflectarrays are planar in nature that are relatively low-cost, easy to fabricate and can realize high gain without using any feeding network [1]. In recent years, dielectric reflectarrays have attracted wide attention in the scientific community due to their low-cost, ease of fabrication, high gain and wide bandwidth [2], [3], [4], [5], [6]. Moreover, they have no conductor losses that will occur in traditional patch-based reflectarrays at THz frequencies [2]. However, most dielectric reflectarrays are using a solid block as a unit cell and the arrays are fabricated with rigid materials, preventing them from being able to transform to a portable or retractable design. As a result, current dielectric reflectarrays require larger volume than microstrip reflectarrays and have a lack of compressibility and deployability. Thus, applicable scenarios for dielectric reflectarrays are extensively limited.

This paper presents a foldable and one-step deployable dielectric reflectarray with high gain and wide bandwidth. The prototype is fabricated with stereolithography (SLA) method utilizing flexible photosensitive resin. The flexible material enables a unique design that facilitates a novel snapping-like mechanism that can be effortlessly folded and deployed to full-scale on-demand using a single-shot deployment technique. These features make it an ideal candidate for various space-limited outer-space and terrestrial applications such as CubeSats, 5G mobile stations, on-body long range communications, etc.

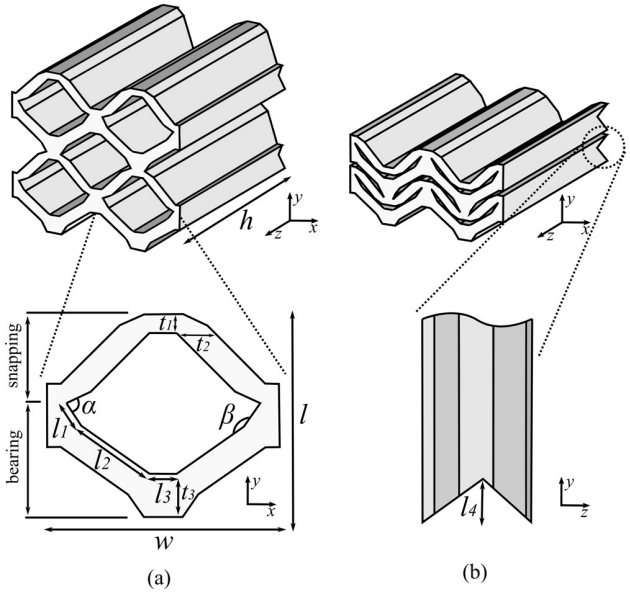

Fig. 1. Unit cell design: (a) deployed structure and top-view of one unit cell; (b) folded structure and side-view of one unit cell. (l_1 = 1mm, l_2 = 3mm, l_3 = 2mm, l_4 = 2mm, α = 80°, β = 160°, t_1 = 0.2mm, t_2 = 0.7mm, t_3 = 2.3mm, w = 8.46mm, l = 7.38mm)

II. Unit Cell

A. Design

The structure of the unit cell is inspired by previous research of both a variation of origami involving cut sections called kirigami [7], as well as mechanical metamaterials [8] in which a tunable tensile snapping structure is printed in a "retracted" configuration. In this work, to ensure an accurate phase-shifting response on each unit cell, the unit cell structure will be carefully designed, optimized and fabricated in a "deployed" configuration. The unit cell design is shown in Fig. 1.

The unit cell consists two segments: snapping segment and bearing segment, the dimension of the structure is defined by four lengths l_1, l_2, l_3, l_4; three dielectric thicknesses t_1, t_2, t_3 and two angles: α, β. One of the key advantage of the proposed design, as compared to a rhomboid structure, is that the proposed structure maintains a constant total width w across stored and fully deployed states, resulting in a Poisson ratio of zero. This is primarily due to angle α and length l_1

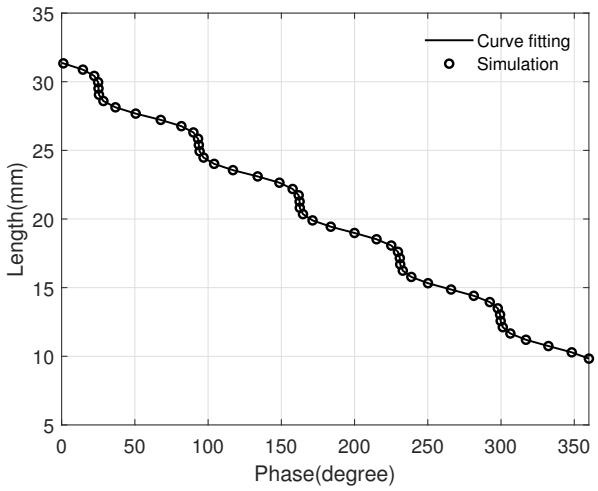

Fig. 2. Unit cell length vs phase shift simulation results.

that create a triangle-shaped hinge which allows the snapping segment "snap" onto the bearing segment. The bottom cut-out with depth l_4 as shown in Fig. 1b is utilized to facilitate a foldable ground plane underneath the reflectarray. The phase of the reflected wave is controlled by varying the height h of the unit cell. The dimension of the unit cell is optimized to display a good foldability at the same time maintain the size less than $1\lambda^2$.

B. Simulation

The unit cell was designed and simulated in CST Studio Suite 2019 frequency domain solver with unit cell boundary condition and Floquet port excitation. The utilized material is Formlabs FLGR02 Flexible photopolymer. This flexible material is a 'rubber-like' elastomer with tensile strength of 7.7-8.5MPa with 8% elongation [9] making it an ideal candidate for deployable dielectric based reflectarrays. Its characterized dielectric constant at 29 GHz is 2.82 with loss tangent 0.0287 utilizing a waveguide WR28 sample with the Nicolson-Ross-Weir NRW methodology. As shown in Fig. 2, the element height h had to be varied from 9.83 mm to 31.10 mm to obtain a full 360° phase shift. The simulation data is processed with a linear interpolative curve fitting algorithm to ensure any desired phase value can be matched with a precise unit cell height.

III. Reflectarray Design, Fabrication and Measurement

A. Reflectarray Design

The designed 3D printed reflectarray configuration shown in Fig. 3a has an offset feed to avoid radiation blockage. The feed horn antenna is placed with a tilted angle θ_a = 20°, the main beam direction is tilted with θ_b = 20° to minimize beam squint. The feed horn antenna aperture has a distance h_a of 120mm away from the center of the reflectarray. The required phase shifting value $\phi(x_i, y_i)$ at any given position (x_i, y_i) can be calculated by (1) and (2),

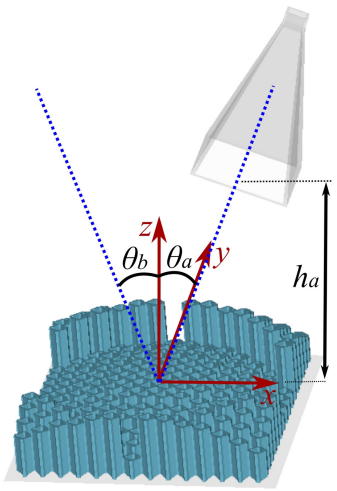

(a)

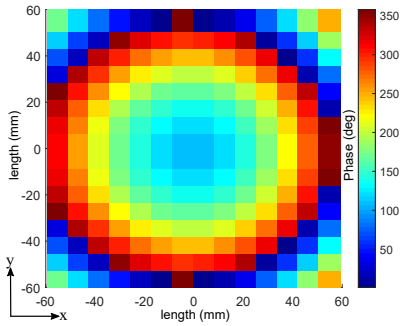

(b)

Fig. 3. Reflectarray design: (a) feed placement and main beam direction; (b) calculated phase-shift distribution.

$$\phi(x_i, y_i) = k_0(d_i - (x_i cos(\varphi_b) + y_i sin(\varphi_b))sin(\theta_b)) \quad (1)$$

$$d_i = \sqrt{(x_i - h_a sin(\theta_b))^2 + y_i^2 + (h_a cos(\theta_b))^2} \quad (2)$$

where k_0 is the propagation constant in vacuum; d_i is the distance between feed horn phase center and element i; φ_b is the main beam steering angle respect to azimuths angle. In this design, φ_b = 0°. The calculated phase-shift distribution is shown in Fig. 3b. The required phase-shift distribution can be realized by placing unit cells with different height h according to the curve fitting result from Fig. 2.

A Visual Basic script is developed to execute in CST Studio Suite 2019 to calculate and generate the dielectric array 3D model. Unit cell dimensions, feed horn placement, beam steering angles, number of elements, etc are all parametrized inside the script for future optimization and scalability. In this work, a 117mm×118mm array with 14×16 elements is utilized. The dimension of this design is limited by the size of 3D printer's build plate, 3D printers with larger printable dimension are commercially available for larger array design.

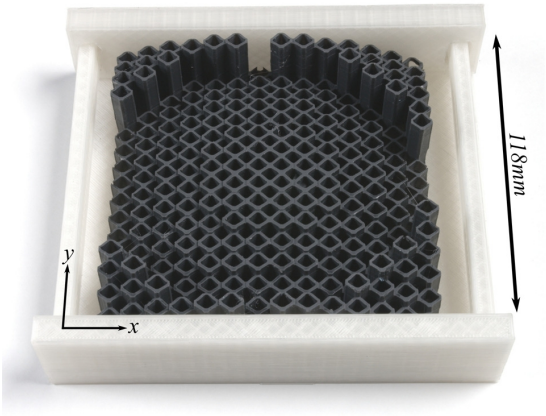

(a)

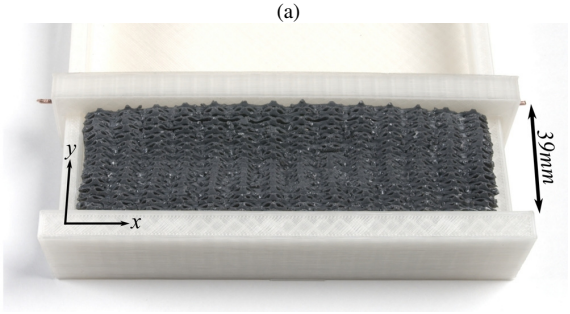

(b)

Fig. 4. Fabricated sample: (a) fully deployed sample (front side); (b) fully retracted sample (back side).

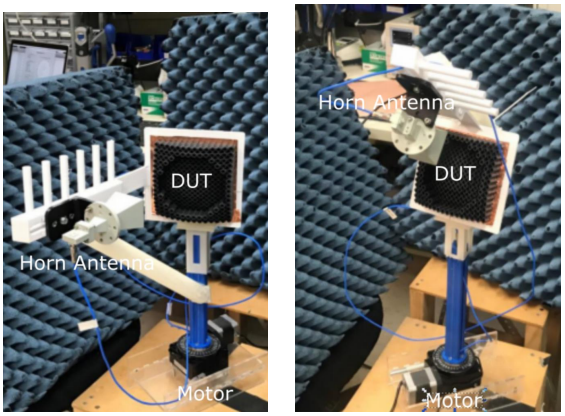

(a) (b)

Fig. 5. Measurement setup: (a) E-plane measurement setup; (b) H-plane measurement setup.

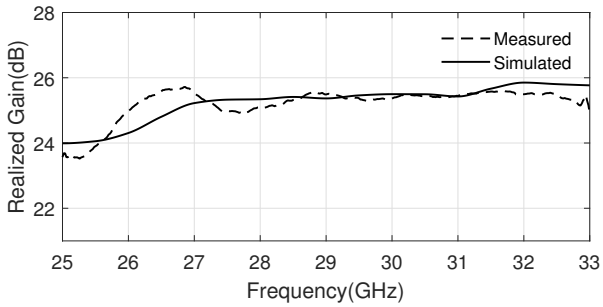

Fig. 6. Gain vs Frequency simulation and measurement results

The performance of the generated dielectric reflectarray is evaluated with full-wave simulation using CST Studio Suite 2019 time domain solver.

B. Fabrication

The dielectric reflectarray prototype was fabricated with Formlabs Form 2 3D printing system. The model was printed with 50μm layer thickness and treated with wash-and-cure post process. The washing process used isopropyl alcohol to remove extra resin left on sample's surface. The curing system utilizes 405nm LED lights and a temperature controlled heater to maximize cross-linking of the photopolymer, in turn increasing structural strength and reducing electromagnetic losses. The post processing recipe was improved from previous work [10] with 10 minutes of washing in 91% isopropyl alcohol, and a final UV cure of 80 minutes at 60°C.

A fully expanded sample is shown in Fig. 4a, and a fully retracted sample is shown in 4b. The reflectarray is folded by a 3D printed frame, the retracted array can be deployed in one-shot with a mechanical switch. The retracted dielectric reflectarray demonstrates a 65% volume reduction in comparison with the fully deployed state.

C. Simulation and Measurement Results

The radiation measurement setup shown in Fig. 5a and Fig. 5b utilize two-antenna method with two AINFO LB-180400-20-C-KF wideband horn antennas.

The plot of realized gain from 25GHz to 33GHz is shown in Fig. 6. The simulation and measurement results matched well with a measured gain of 25.5dBi at 29GHz along with a simulated gain of 25.4dBi. The measured 1dB bandwidth is 16.34% with simulated 1dB bandwidth of 18.75%. The performance comparison of state-of-art dielectric reflectarrays at similar frequency ranges is shown in Table 1, the proposed reflectarray shows promising performance with deployability.

Fig. 7a and Fig. 7b show a good match between measured and simulated radiation pattern with co-polarization antenna placement. The simulation achieves 6.1° half power beamwidth (HWBW) with sidelobe level (SLL) of -18.30dB on E-plane, 11.1° HWBW with SLL of -20.11dB on H-plane. While the fabricated sample measures a 6.0° HWBW with -17.37dB SSL on E-plane, 10.5° HWBW with -20.54dB SLL on H-plane.

Fig. 7c and Fig. 7d show the results of measured and simulated radiation pattern with cross-polarization antenna placement. The simulation achieves 6.0° HWBW with SLL of -17.20dB on E-plane, 10.2° HWBW with SLL of -19.92dB on H-plane. While the fabricated sample measures a 6.0° HWBW with -15.27dB SSL on E-plane, 9.3° HWBW with -19.44dB SLL on H-plane.

The measured radiation pattern shows slightly increased SLL, this is mainly limited by 3D printer's maximum resolution. Photopolymer tends to be over-cured with long

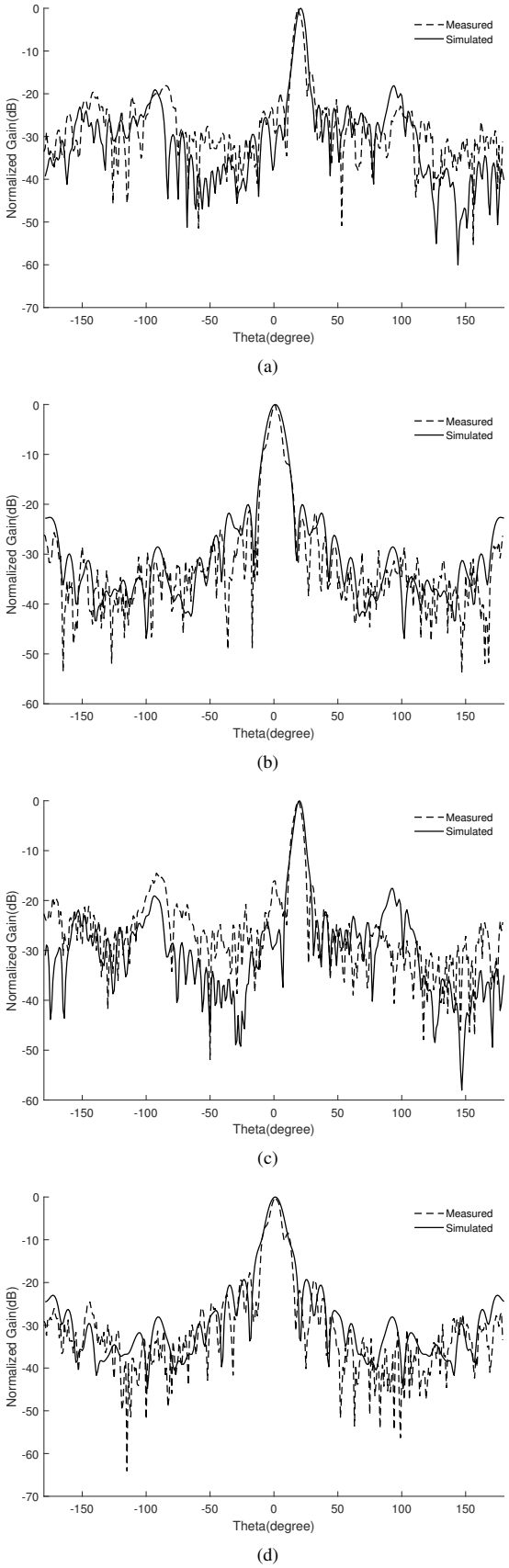

Fig. 7. Measured Radiation Pattern: (a) E-plane co-polarization; (b) H-plane co-polarization; (c) E-plane cross-polarization; (d) H-plane cross-polarization.

Table 1. Comparasion with state-of-art dielectric reflectarrays.

Design	Fabrication	Freq	Size	Gain	BW	Deploy
[4]	PCB Etching	35GHz	$153.9\lambda^2$	23.9dB	NA	N
[5]	3D Printing	30GHz	$144.0\lambda^2$	28.0dB	10.0%	N
[6]	Monolithic	31GHz	$154.0\lambda^2$	28.3dB	5.2%	N
Proposed	3D Printing	29GHz	$129.3\lambda^2$	25.5dB	16.3%	Y

tube-shaped structure, causing the printed sidewall to be thicker than intended. This challenge can potentially be solved with newer 3D printing technique such as linear illumination in which the laser beam always perpendicular to the build plate.

IV. Conclusion

This paper demonstrated the first-of-its-kind one-shot deployable reflectarray inspired by kirigami structures and mechanical metamaterials. The design is realized through low-cost commercialized 3D printing system with flexible materials. The fabricated prototype shows high realized gain, wide-bandwidth and 65% of volume reduction when retracted, enables more space-limited communication applications for dielectric reflectarrays. The flexible unit cell structure can potentially introduce multi-stage reconfigurability to the design of dielectric reflectarray in future work.

Acknowledgment

The authors would like to thank National Science Foundation (NSF) for supporting this work.

References

[1] J. Huang, *Reflectarray Antennas*. Wiley-IEEE Press, oct 2007. [Online]. Available: https://www.xarg.org/ref/a/047008491X/

[2] P. Nayeri, M. Liang, R. A. Sabory-Garcıa, M. Tuo, F. Yang, M. Gehm, H. Xin, and A. Z. Elsherbeni, "3d printed dielectric reflectarrays: Low-cost high-gain antennas at sub-millimeter waves," *IEEE Transactions on Antennas and Propagation*, vol. 62, no. 4, pp. 2000–2008, April 2014.

[3] R. Deng, F. Yang, S. Xu, and M. Li, "Radiation performances of conformal dielectric reflectarray antennas at sub-millimeter waves," in *2016 IEEE International Conference on Microwave and Millimeter Wave Technology (ICMMT)*, vol. 1, June 2016, pp. 217–219.

[4] Y. Sun and K. W. Leung, "Millimeter-wave substrate-based dielectric reflectarray," *IEEE Antennas and Wireless Propagation Letters*, vol. 17, no. 12, pp. 2329–2333, Dec 2018.

[5] S. Zhang, "Three-dimensional printed millimetre wave dielectric resonator reflectarray," *IET Microwaves, Antennas Propagation*, vol. 11, no. 14, pp. 2005–2009, 2017.

[6] M. h. Jamaluddin, R. Sauleau, X. Castel, R. Benzerga, L. Coq, R. Gillard, and T. Koleck, "Design, fabrication and characterization of a dielectric resonator antenna reflectarray in ka-band," *Progress In Electromagnetics Research B*, vol. 25, pp. 261–275, 01 2010.

[7] T. Castle, D. M. Sussman, M. Tanis, and R. D. Kamien, "Additive lattice kirigami," *Science Advances*, vol. 2, no. 9, 2016. [Online]. Available: https://advances.sciencemag.org/content/2/9/e1601258

[8] A. Rafsanjani, A. Akbarzadeh, and D. Pasini, "Snapping mechanical metamaterials under tension," *Advanced Materials*, vol. 27, p. 5931, 10 2015.

[9] [Online]. Available:https://support formlabs com/s/article/Using-Flexible-Resin

[10] Y. Cui, S. A. Nauroze, and M. M. Tentzeris, "Novel 3d-printed reconfigurable origami frequency selective surfaces with flexible inkjet-printed conductor traces," in *2019 IEEE MTT-S International Microwave Symposium (IMS)*, June 2019, pp. 1367–1370.